Study of Solidification Features of Nickel-Base Superalloys in Relation with Composition

J. LECOMTE-BECKERS

The influence of the six major alloying elements: carbon, chromium, cobalt, molybdenum, titanium, and aluminum on the solidification sequence of nickel-base superalloys was investigated. The microstructure was found to depend greatly on aluminum and titanium contents. During solidification the liquid is enriched in titanium and molybdenum, whereas the dendrite cores are richer in cobalt. Aluminum and chromium segregate in the liquid or in the dendrite center, depending on alloy nominal composition. Chemical analysis of the carbides showed that their composition changes during solidification, thus affecting the composition of the residual liquid. The composition of carbides is strongly influenced by titanium and molybdenum nominal content in the alloy. Statistical analysis of the transformation temperatures obtained by DTA showed that titanium and aluminum influence the entire solidification sequence.

I. INTRODUCTION

THIS research is concerned with the analysis of the solidification behavior of a nickel-base superalloy, and the effect of alloy composition thereon. IN100 was selected for this investigation. This alloy contains large amounts of aluminum and titanium, the sum of which is the highest encountered in today's superalloys. Also, this alloy is characterized by a high percentage (more than 60 pct) of the strengthening phase γ'-Ni_3 (Al, Ti), and consequently it has a high specific strength. Furthermore, this alloy exhibits some negative features, such as structural instability due to the sigma phase precipitation and susceptibility to microporosity formation. Many experiments during the past two decades have focused on ways to overcome these difficulties, for example by modifying the chemical composition. Moreover, recent studies have shown the important role played by the solidification sequence in the formation of microporosity.[1] In the present work, the technique of factorial design has been used to study the influence on the solidification sequence of the six major alloying elements: carbon, chromium, cobalt, molybdenum, titanium, and aluminum.

The cast microstructure of IN100 normally consists of coherent γ' precipitates in a γ dendritic matrix with carbide particles (MC-type) distributed along or between the dendrite arms as well as grain boundaries and the γ-γ' eutectic generally occupying the interdendritic regions. Dendritic growth in nickel superalloys gives rise to microsegregation which greatly affects the formation and distribution of various secondary phases in the as-cast alloy. The occurrence of the γ-γ' eutectic regions is a result of this microsegregation.

The present investigation was mainly concerned with the influence of the above-mentioned six alloying elements on the cast microstructure (morphology of the γ' precipitates, carbides and eutectic, dendrite density, carbide composition), on the formation temperature of the various phases, and dendritic and interdendritic segregation.

J. LECOMTE-BECKERS is Senior Research Associate, Department of Metallurgy and Materials Science, University of Liège, Belgium.

Manuscript submitted February 26, 1987.

II. EXPERIMENTAL PROCEDURE

A. *Choice and Preparation of the Alloys*

Eight experimental compositions were chosen following factorial design of 2^3 experiments to study the influence of the six major elements, each used at only two nominal contents (Table I). The elements carbon, chromium, and cobalt have been chosen as main factors, and the elements molybdenum, titanium, and aluminum have been identified with the two-factor interactions. The three-factor interaction was used to estimate σ, the experimental error. Statistical significance of the element effects was tested by an F-test (analysis of variance) and the level of significance of the effects was fixed at 10 pct. The significant effects were hatched in the different graphs and the experimental error σ is indicated.

The experimental alloys were elaborated under vacuum in an induction furnace. After homogenization, the liquid alloys were cast into preheated cylindrical sillimanite molds. These cylindrical rods were used for microstructural characterizations and DTA measurements. They were also subsequently turned to adequate specimen dimensions for QDS experiments.

B. *Directionally Solidified and Quenched Samples*

The major part of this investigation was conducted on directionally solidified and quenched samples (Q.D.S.). This technique of unidirectional growth interrupted by quenching of the remaining liquid at a given moment offers a convenient way of studying the microstructure of the solid during solidification, as well as after its completion. It allows a fairly easy control of the two important parameters: thermal gradient and solidification rate.

The turned sample was contained in an alumina crucible (0.006 m diameter × 0.015 m long) which is placed on a bottom water-cooled chill. This assembly was withdrawn at a constant rate R (0.060 mh^{-1}) from an induction furnace equipped with a graphite susceptor. The temperature of the sample was recorded by a second thermocouple placed at the central axis of the sample, in the solidified part which will be melted and unidirectionally solidified.

Table I. Factorial Design

Experiments	A Pct C	B Pct Cr	C Pct Co	C(= AC) Pct Mo	E(= AC) Pct Ti	F(= BC) Pct Al	Alloy Number	Element Tested
1 (def)	0.06	7.9	0	4	4.6	5.4	I	—
a (f)	0.14	7.5	0	0.5	1	5.5	II	carbon
b (e)	0.05	12	0	0.5	4.7	2.2	III	chromium
ab (d)	0.14	11.7	0	4	1	2.2	IV	molybdenum
c (d)	0.05	7.7	11.7	4	1	2.0	V	cobalt
ac (e)	0.15	8	10.2	0.5	4.6	2	VI	titanium
bc (f)	0.04	11.7	10.3	0.6	1.1	4.8	VII	aluminum
abc (def)	0.16	12	10.7	3.9	4.6	5.1	VIII	—

The sample was melted under vacuum and superheated by 120 °C above the equilibrium temperature, which was determined by DTA. After the temperature equilibrium was attained the crucible was withdrawn.

When steady state was established the larger of the mushy zone as well as the temperature profile in the sample was stationary with respect to the furnace and the growth rate of the solid in the heat flow was equal to the rate at which the crucible was withdrawn. The average thermal gradient in the solid-liquid region was determined from the temperature-distance charts and was 1×10^4 Km^{-1}. Under these steady-state growth conditions, solidification was dendritic. Growth of the dendritic specimen was interrupted at a given moment by quenching the remaining liquid achieved by pneumatically pulling the crucible from the furnace at very high speed (1 m/s) and simultaneously cooling it with the helium jet.

C. *Metallographic Preparation*

Each directionally solidified sample was sectioned longitudinally, polished, and etched to measure the length of the dendrites. Plane transverse sections perpendicular to the heat-flow direction taken within the mushy zone from the top to the bottom of the dendrites were used for studying morphological features and microsegregation at various temperatures between the liquidus and the solidus of the alloy.

Morphological analyses were performed on transverse sections after appropriate etching on a (Quantimet 720) computerized image analyzer. Forty-nine fields were analyzed on each section. Each field (7×5 mm^2) corresponded to 500,000 pixels. Quantitative microsegregation measurements were performed on transverse sections on a (Cambridge) scanning electron microscope with EDS detectors.

The specimen was slightly etched with aqua regia to reveal the dendritic structure. Ten measurements were taken with an expanded beam at different locations in the center or the surface of the dendrites or in the interdendritic region (Figure 1). Ten point measurements were also made on the carbides. All microprobe analyses were performed by point counting integrating for 100 seconds, using a standard of Ni to normalize the number of counts. ZAF corrections *via* Magic V (computer program which eliminates stray fluorescence peaks, smooths out the spectra, takes the noise away, and corrects peak intensities for atomic number effects, absorption, and fluorescence) were used with standards under constant operating conditions: incidence angle: 45 deg, emergence angle: 47.2 deg, and operating voltage: 20 kV.

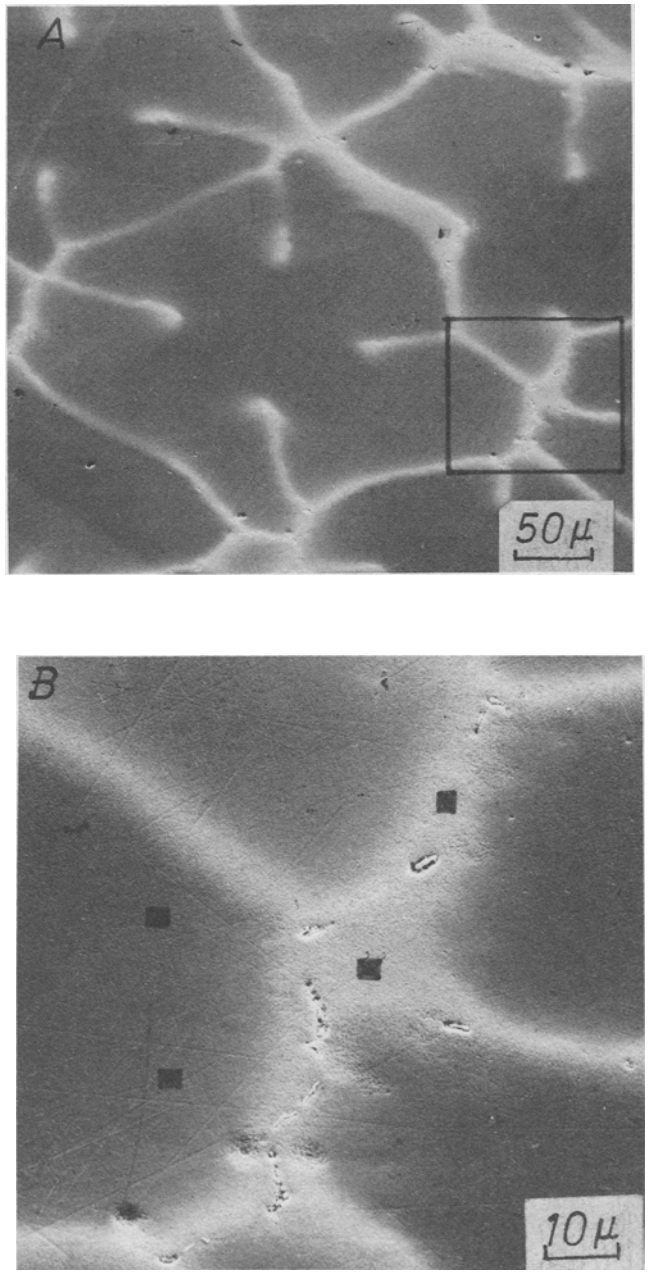

Fig. 1—(*a*) General view of a dendrite (SEM). (*b*) Example of measurement locations in the interdendritic region (white) or in the board of the dendrite.

D. *Differential Thermal Analysis*

Small cubic samples, approximately 0.3 g in weight, were taken from each master rod and subjected to Differential Thermal Analysis (DTA) against a Pt reference. The tests were carried out under the protection of a constant argon flow (300 ml/min) at three constant heating and cooling rates (15 °C/min, 10 °C/min, 7 °C/min, peak temperature of 1450 °C) to observe the solidification sequence.

III. RESULTS AND DISCUSSION

A. *Microstructural Examination*

This examination was performed on the master rods.

The experimental alloys can be divided into three groups: A, B, and C, following their microstructures.

(A) alloys containing interdendritic MC carbides, γ-γ' eutectic, and γ' precipitates in the dendritic γ matrix (Figure 2) (alloys I and VIII);
(B) alloys containing interdendritic MC carbides and γ' precipitates in γ matrix (Figure 3) (alloys II, III, VI, VII); and
(C) alloys containing only MC or $M_{23}C_6$ carbides in the γ matrix (Figure 4) (alloys IV and V).

These different microstructures can be easily explained when considering the aluminum and titanium contents. Alloys with low Al and Ti contents show a supersaturated γ matrix. When Al and Ti contents increase, γ' precipitates in the γ matrix. Finally, when the (Al + Ti) content is sufficiently high, the γ-γ' eutectic precipitates at the end of the solidification process.

B. *Differential Thermal Analysis*

Transformation temperatures measured on cooling of master rods from the liquid state at different rates differ from one alloy to the other; the different transformation peaks analyzed correspond well to the different phases observed in the microstructure. Figure 5 illustrates a typical curve.

To compensate peak broadening, an extrapolation method was used to determine the onset of a transition.[2] The onset temperature is the point at which the extrapolated baseline intersects the tangent drawn at the point of greatest slope on the leading edge of the peak. The completion of a transition occurs somewhere along the training edge of the peak, between the maximum and the return to baseline. When the trailing edge of a peak is steep, the temperature at the peak maximum may be used as a reasonable approximation of the

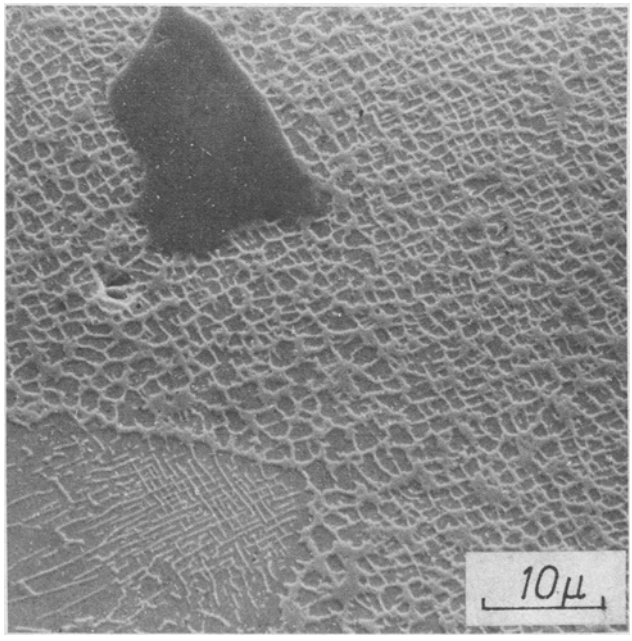

Fig. 2—Group A alloy microstructure (SEM).

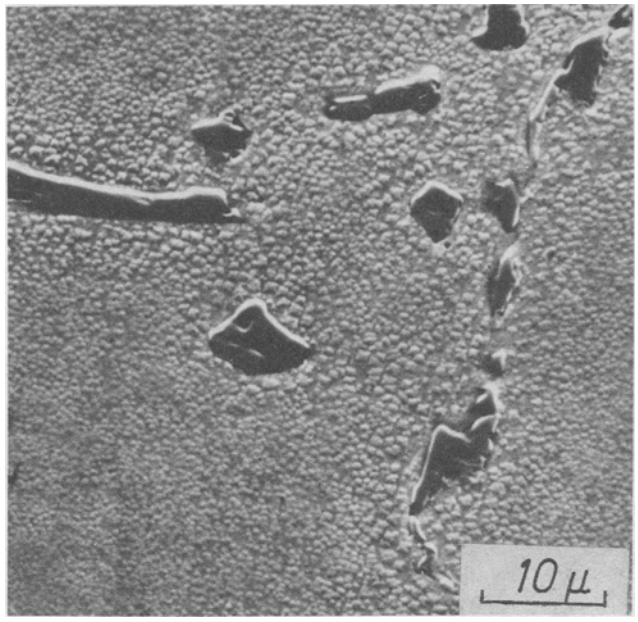

Fig. 3—Group B alloy microstructure (SEM).

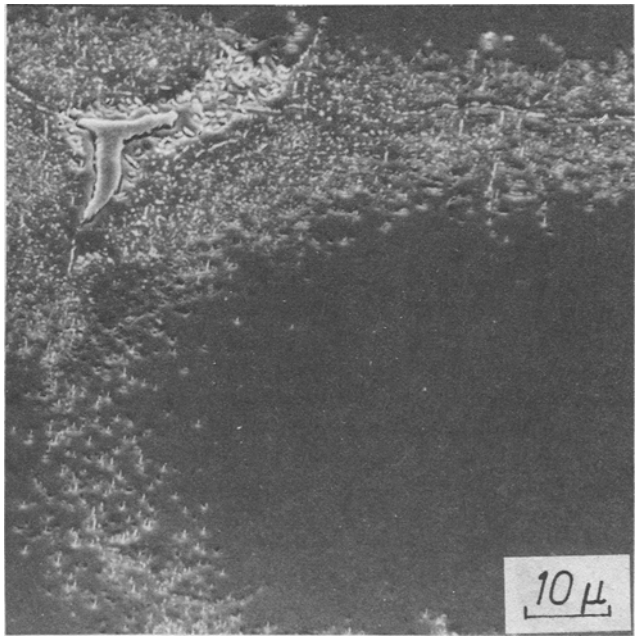

Fig. 4—Group C alloy microstructure (SEM).

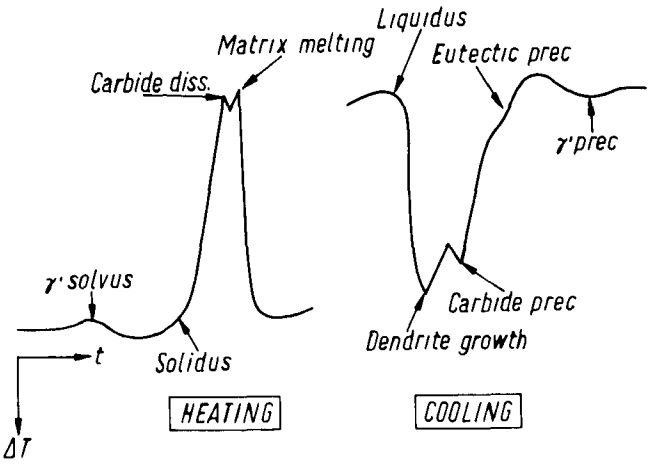

Fig. 5—Typical DTA curve.

completion temperature.[3] However, when the trailing edge of a peak is smooth, indicating that the transformation is slowing down before finishing, the completion is taken at the point at which the extrapolated baseline intersects the tangent drawn at the point of greatest slope on the trailing edge of the peak.

Three cooling and heating rates were chosen, in order to extrapolate the transformation temperatures to zero cooling, thus defining an intrinsic equilibrium transformation temperature. Each experiment was repeated three times and the average was calculated and used to obtain the equilibrium temperature (Figure 6). This temperature was used to define the superheating for QDS samples.

Statistical analyses have been made to assess the effect of chemical composition on the different equilibrium transformation temperatures during cooling.

Titanium, aluminum, chromium, and molybdenum have a significant effect on the equilibrium liquidus temperature (Figure 7). An increase in their contents decreases T_L. The effect was the more important for aluminum and titanium. Aluminum, titanium, and chromium influence significantly the equilibrium solidus temperature (Figure 8). An increase in their content decreases T_S. Carbon, aluminum, and titanium have a significant effect on the equilibrium solidification range (Figure 9). An increase in their contents increases

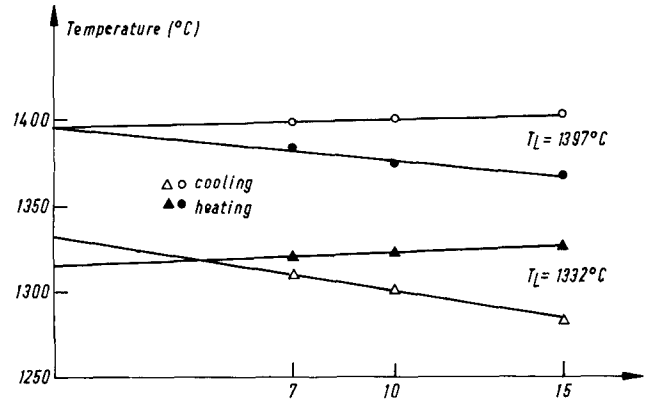

Fig. 6—Extrapolation method used to determine equilibrium transformation temperatures (zero cooling rate).

Table II. Multiple Correlation for T_L

Elements	Coefficients	Standard Deviation/ Coeff.	t. Student	Q(F)
Aluminum	−13.47	1.68	− 9.54	0.066
Cobalt	− 0.72	5.74	− 1.74	0.332
Chromium	− 4.51	2.18	− 4.19	0.149
Molybdenum	− 3.39	1.84	− 2.66	0.229
Titanium	−14.58	1.92	−11.82	0.054
Carbon	13.40	0.05	0.29	0.819
Constant	1530.54			
Multiple correlation coefficient		0.998		
Residual standard deviation		6.19		

Table III. Multiple Correlation for T_S

Elements	Coefficients	Standard Deviation/ Coeff.	t. Student	Q(F)
Aluminum	− 18.35	1.68	−6.03	0.105
Cobalt	− 1.30	5.74	−1.46	0.382
Chromium	− 6.09	2.18	−2.62	0.232
Molybdenum	− 1.67	1.84	−0.61	0.653
Titanium	− 16.29	1.91	−6.13	0.103
Carbon	−151.97	0.05	−1.54	0.366
Constant	1521.768			
Multiple correlation coefficient		0.994		
Residual standard deviation		13.34		

Table IV. Multiple Correlation for ΔT

Elements	Coefficients	Standard Deviation/ Coeff.	t. Student	Q(F)
Aluminum	4.66	1.68	2.45	0.247
Cobalt	0.51	5.74	0.91	0.530
Chromium	1.73	2.18	1.19	0.445
Molybdenum	−1.92	1.84	−1.12	0.465
Titanium	1.93	1.92	1.16	0.453
Carbon	158.27	0.05	2.57	0.237
Constant	9.3			
Multiple correlation coefficient		0.97		
Residual standard deviation		8.35		

Table V. Multiple Correlation for T_C

Elements	Coefficients	Standard Deviation/ Coeff.	t. Student	Q(F)
Aluminum	− 9.54	1.68	−2.32	0.259
Cobalt	0.11	5.74	0.09	0.944
Chromium	− 2.30	2.18	−0.73	0.597
Molybdenum	0.28	1.84	0.08	0.951
Titanium	− 13.82	1.92	−3.85	0.162
Carbon	−147.28	0.05	−1.17	0.468
Constant	1450.25			
Multiple correlation coefficient		0.98		
Residual standard deviation		18.04		

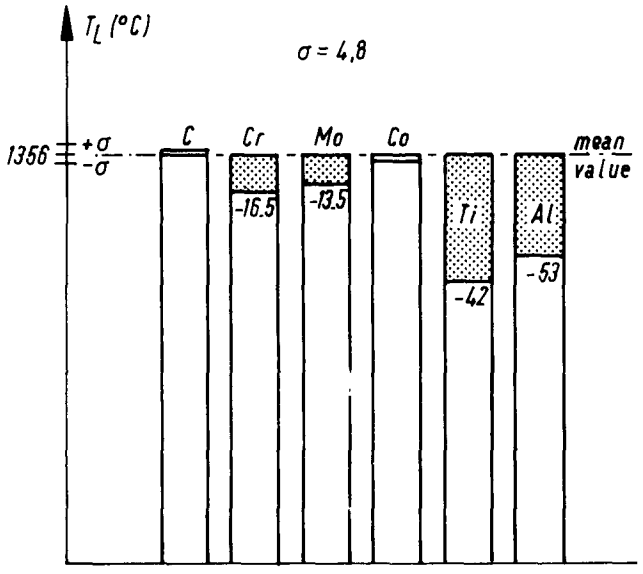

Fig. 7—Effect of alloying elements on equilibrium liquidus temperature.

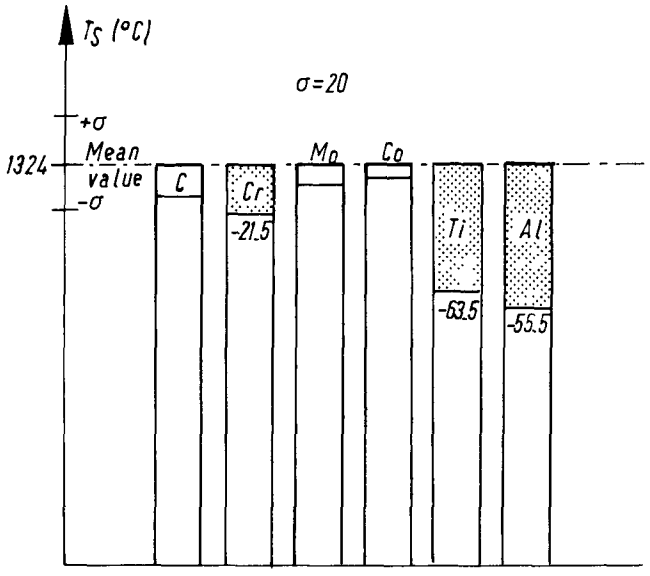

Fig. 8—Effect of alloying elements on equilibrium solidus temperature.

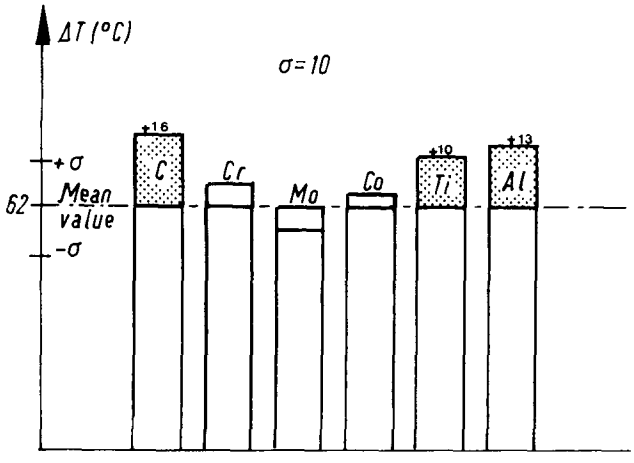

Fig. 9—Effect of alloying elements on equilibrium solidification range.

ΔT. Titanium and aluminum influence significantly the equilibrium carbide temperature formation (Figure 10). An increase in their contents decreases T_C.

The following relations between equilibrium transformation temperature and alloy composition were deduced (Tables II to V):

$$T_L = 1530.54 - 13.47[\text{Al}] - 0.72[\text{Co}] - 4.51[\text{Cr}] - 3.39[\text{Mo}] - 15.58[\text{Ti}] + 13.40[\text{C}] \quad [1]$$

$$T_S = 1521.77 - 18.35[\text{Al}] - 1.30[\text{Co}] - 6.09[\text{Cr}] - 1.67[\text{Mo}] - 16.29[\text{Ti}] - 151.97[\text{C}] \quad [2]$$

$$\Delta T = 9.30 - 4.66[\text{Al}] + 0.51[\text{Co}] + 1.73[\text{Cr}] - 1.92[\text{Mo}] + 1.93[\text{Ti}] + 158.27[\text{C}] \quad [3]$$

$$T_C = 1450.25 - 9.54[\text{Al}] + 0.11[\text{Co}] - 2.30[\text{Cr}] + 0.28[\text{Mo}] - 13.82[\text{Ti}] - 147.28[\text{C}] \quad [4]$$

The terms in [ ] are the weight percentages.

Equation [1] is slightly different from that obtained by Cook and Guthrie[4] for IN100 alloy for a cooling rate of 10 °C/min:

$$T_L(°\text{C}) = 1508 - 258[\text{B}] - 51.5[\text{C}] - 32.5[\text{Zr}] - 17[\text{Ti}] - 11.9[\text{Al}] - 4.84[\text{Mo}] - 2.41[\text{Cr}] - 1.63[\text{V}] + 0.72[\text{Co}]$$

This can be explained by the differences in alloying element contents and in cooling rates. Meanwhile, the coefficients for the most important factors (aluminum, chromium, molybdenum, titanium) are similar.

C. *Morphological Analyses*

1. *Dendrite number density*

Morphological features of the mushy zone of QDS samples can be characterized by the number of dendrites/unit surface area, n_p, on transverse sections near the liquidus

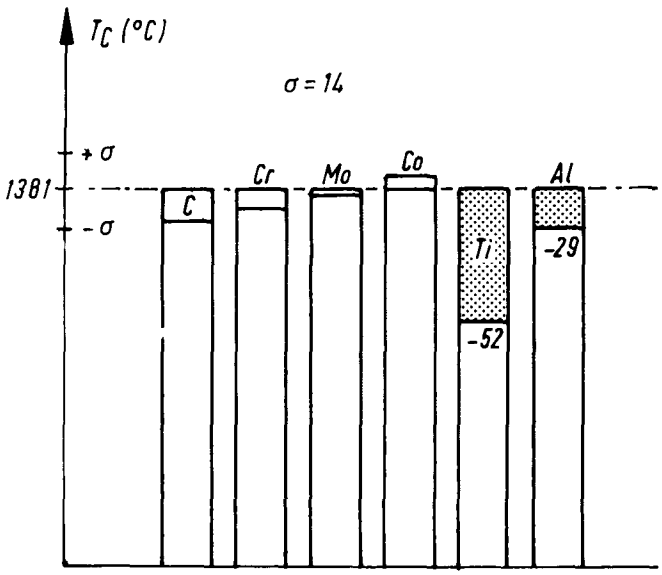

Fig. 10—Effect of alloying elements on equilibrium carbide temperature formation.

temperatures (T_L − 10 °C). This dendrite number density, n_p, is related to the interdendritic primary spacing by the relation

$$\lambda_p = n_p^{-1/2}.$$

Factorial analysis of n_p shows that an increase in titanium decreases n_p and increases the interdendritic primary spacing (Figure 11).

2. *γ-γ′ eutectic*

Eutectic regions are found only in the two alloys, I and VIII, rich in aluminum and titanium. Their number and size are more important in alloy VIII (than in alloy I) (Table VI). The fact can be related to the higher chromium and cobalt contents in alloy VIII which move the eutectic valley.

3. *Carbides*

Carbon and titanium affect carbide number density (Figure 12). Carbide size is influenced by molybdenum, titanium, and aluminum. The effects of carbon, titanium, and molybdenum are quite understandable because these are carbide forming elements. The effect of aluminum is related to segregation and effective partition ratio K, as we will see hereafter.

D. *Carbide Composition*

EDS analyses of carbides at different locations from the dendrite tips indicate that their composition evolves during solidification (Table VII). Carbide composition at the beginning of solidification is related to the alloy nominal composition. During solidification the titanium and molybdenum contents in the melt evolve independently. At the end of solidification, carbides are always richer in titanium than in molybdenum independently of the alloy nominal composition.

E. *Dendritic Microsegregation*

Solute concentration was measured for each alloy by EDS on transverse sections at the dendrite center, dendrite surface,

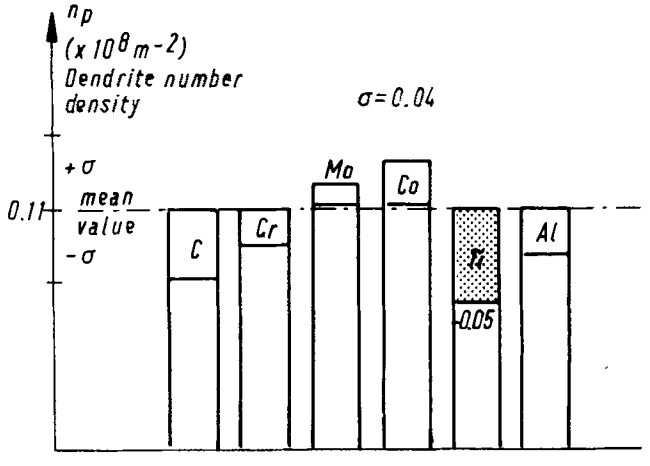

Fig. 11 — Effect of alloying elements on dendrite number density.

Table VI. Eutectic Region Features

Alloy	(Pct)	Number Density (mm^{-2})	Mean Surface (μ^2)
I	0.071	6.5	47.1
VIII	2.336	71.15	96

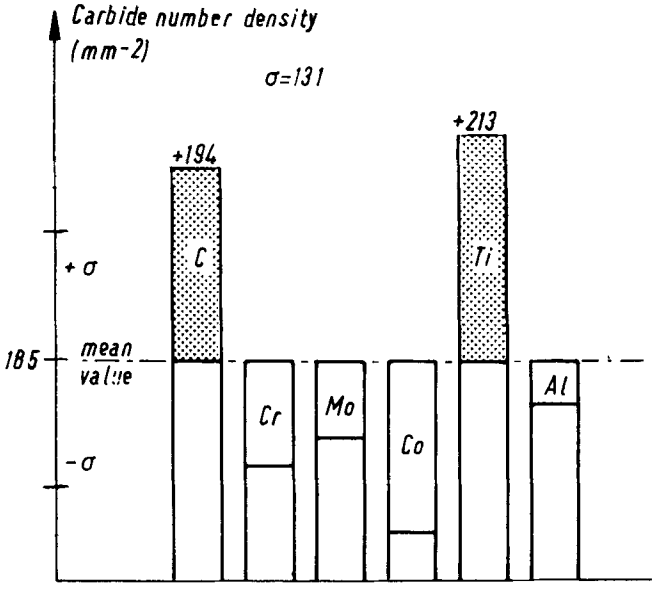

Fig. 12 — Effect of alloying elements on carbide number density.

Table VII. Chemical Analysis of Carbides

Nominal Alloy Content	Alloy	Carbide Analysis	
4 pct Mo-4.5 pct Ti	VIII	begin of sol.	$(Ti_{0.51}\text{-}Mo_{0.49})C$
		end of sol.	$(Ti_{0.62}\text{-}Mo_{0.38})C$
	I	end of sol.	$(Ti_{0.61}\text{-}Mo_{0.39})C$
0.5 pct Mo-4.5 pct Ti	III	begin of sol.	$(Ti_{0.96}\text{-}Mo_{0.04})C$
		end of sol.	$(Ti_{0.92}\text{-}Mo_{0.08})C$
	VI	begin of sol.	$(Ti_{0.96}\text{-}Mo_{0.04})C$
		end of sol.	$(Ti_{0.92}\text{-}Mo_{0.08})C$
4 pct Mo-1 pct Ti	IV	begin of sol.	$(Ti_{0.45}\text{-}Mo_{0.55})C$
		end of sol.	$(Ti_{0.58}\text{-}Mo_{0.42})C$
	V	begin of sol.	$(Ti_{0.48}\text{-}Mo_{0.52})C$
		end of sol.	$(Ti_{0.54}\text{-}Mo_{0.46})C$
0.5 pct Mo-1 pct Ti	II	begin of sol.	$(Ti_{0.81}\text{-}Mo_{0.19})C$
		end of sol.	$(Ti_{0.8}\text{-}Mo_{0.2})C$
	VII	begin of sol.	$(Ti_{0.8}\text{-}Mo_{0.2})C$
		end of sol.	$(Ti_{0.8}\text{-}Mo_{0.2})C$

and interdendritic liquid. The effective partition ratio K (ratio of concentrations of a given element in the solid dendrite center and in the interdendritic liquid phases) was calculated at the beginning of solidification (first value) and at the end (second value).

The results obtained indicate that there is a concentration gradient between the center of the dendrite, the dendrite surface, and the interdendritic regions.

The liquid is always enriched in titanium and molybdenum. On the contrary, in the cobalt-containing alloys, the center of the dendrite is always richer in cobalt than the liquid. Chromium segregation depends on aluminum content in the alloy. In alloys lean in aluminum, the dendrite cores are enriched with chromium. On the other hand, in alloys rich in aluminum, the dendrite cores exhibit a lower chromium concentration than the liquid. A comparable behavior is observed with aluminum: all alloys do not exhibit the same behavior. In alloys rich in aluminum, the liquid is richer in

aluminum than the solid. In alloys poor in aluminum the liquid is poorer than the solid.

During solidification the solute redistribution at the interface leads to variations of the liquid composition and consequently the partition ratio varies. This evolution is rather important for titanium and molybdenum, especially because during solidification carbides with different titanium over molybdenum content ratio precipitate.

Factorial analysis conducted on effective partition ratios at the end of solidification indicates that interactions exist between the elements (Table VIII).

The effective partition ratio K_{Al} is significantly influenced by aluminum, chromium, and carbon contents. An increase in aluminum and chromium contents decreases K_{Al}; an increase in carbon content increases it (Figure 13).

The effective partition ratio K_{Cr} is significantly influenced by aluminum, molybdenum, chromium, and cobalt. It decreases with an increase in aluminum and molybdenum contents; it increases with an increase in chromium and cobalt contents (Figure 14).

The effective partition ratio K_{Ti} is significantly influenced by molybdenum, titanium, and aluminum. It decreases with an increase in titanium and aluminum contents; it increases with an increase in molybdenum content (Figure 15).

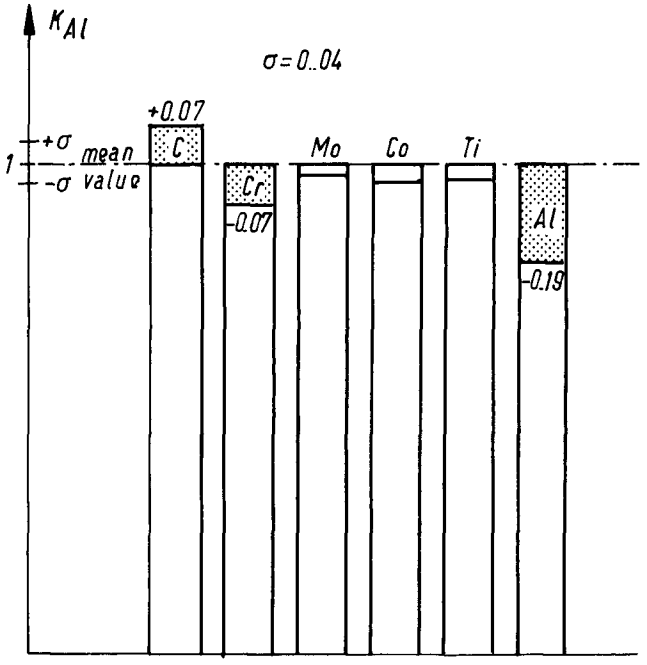

Fig. 13—Effect of alloying elements on effective partition ratio of Al.

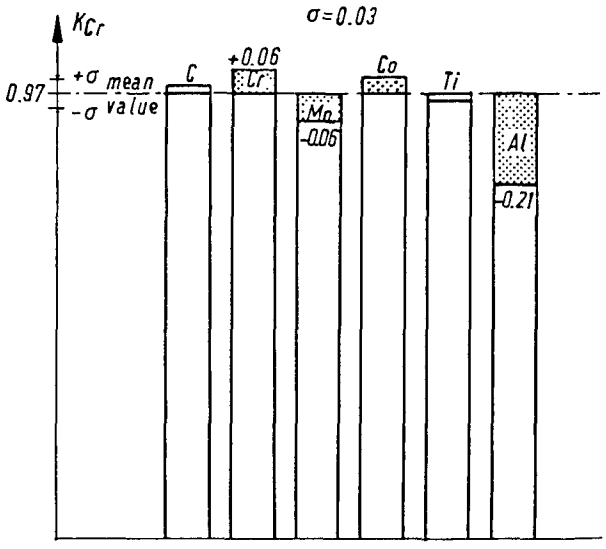

Fig. 14—Effect of alloying elements on effective partition ratio of Cr.

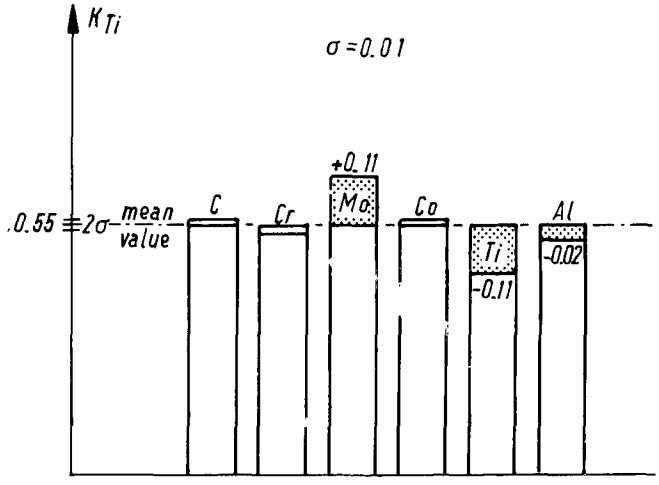

Fig. 15—Effect of alloying elements on effective partition ratio of Ti.

IV. CONCLUSIONS

1. Statistical analysis of the intrinsic equilibrium transformation temperatures determined by DTA showed that
   a. an increase in carbon content brings about an increase in ΔT (solidification range),

Table VIII. Partition Ratio $K = C_S/C_L$

Alloy	K_{Al}	K_{Cr}	K_{Mo}	K_{Co}	K_{Ti}
I	0.93	0.86 to 0.75	0.81 to 0.73	—	0.62 to 0.52
II	0.99	0.94 to 0.86	—	—	0.32 to 0.52
III	1.07	1.11	—	—	0.42
IV	1.10	1.07	0.35 to 0.5	—	0.60 to 0.65
V	1.06	1.04	0.85	1.05	0.60 to 0.65
VI	1.23 to 1.19	1.10	—	1.15	0.46
VII	0.75 to 0.82	0.95	—	1.17	0.32 to 0.52
VIII	0.99 to 0.89	0.93 to 0.89	0.90 to 0.80	1.02	0.62 to 0.52

b. an increase in chromium content brings about a decrease in T_L (liquidus temperature) and T_S (solidus temperature),
c. an increase in molybdenum content reduces T_L,
d. an increase in titanium contents leads to a decrease of T_L, T_S, and T_C (carbide formation temperature) and to an increase of ΔT,
e. an increase in aluminum content decreases T_L, T_S, and T_C and increases ΔT, and
f. an increase in cobalt content has no effect on these temperatures.

2. An increase in titanium content decreases the number density of dendrites and hence increases the interdendritic primary spacing.
3. During solidification, liquid is always enriched with titanium and molybdenum. Dendrite center is enriched with cobalt in alloy containing this element. Aluminum and chromium segregate in the liquid or in the dendrite center following alloy nominal composition. The effective solid-liquid partition coefficient for titanium and molybdenum is less than one. That of cobalt is higher than one. That of aluminum and chromium depends on alloy nominal composition. Segregation of aluminum depends on aluminum, chromium, and carbon contents. That of chromium depends on chromium, cobalt, molybdenum, and aluminum contents. That of titanium one depends on titanium, molybdenum, and aluminum contents. That of cobalt is influenced by molybdenum content and conversely.
4. Carbide composition changes during solidification and is strongly influenced by the titanium and molybdenum contents. At completion of solidification carbides are always richer in titanium than in molybdenum. The carbide number density is influenced by carbon and titanium; their size depends on carbon, titanium, and aluminum contents.

ACKNOWLEDGMENTS

The author expresses her deep gratitude to CRM (Centre de Recherches Métallurgiques–Belgique) and IRSIA (Institut pour la Recherche Scientifique dans l'Industrie et l'Agriculture–Belgique) for support of this work. A sincere appreciation is extended to Dr. D. Coutsouradis and particularly to Dr. M. Lamberigts of CRM for providing support and valuable comments. Thanks are also due to Professor T. Z. Kattamis, University of Connecticut for helpful discussions.

REFERENCES

1. L. Ouichou: *Proc. of High Temperature Alloys for Gas Turbines 82*, D. Reidel Publ. Co., Dordrecht, The Netherlands, 1982, pp. 995-71.
2. G. E. Maurer, J. Domingue, and W. J. Boesch: *Proc. of the 27th Annual Meeting of the Investment Casting Institute*, 1979, pp. 1601-23.
3. C. J. Burton: *Superalloys: Metallurgy and Manufacture, Proc. of the 3rd Int. Symposium*, Claitor's Pub. Div., Baton Rouge, LA, 1976, pp. 147-57.
4. R. M. Cook and A. M. Guthrie: *Foundry Trade Journal*, May 1966, pp. 686-89.